Published in final edited form as:
Dev Neurobiol. 2012 September ; 72(9): 1213–1228. doi:10.1002/dneu.20988.

Members of the BMP, Shh and FGF morphogen families promote chicken statoacoustic ganglion neurite outgrowth and neuron survival *in vitro*

Kristen N. Fantetti and **Donna M. Fekete***
Department of Biological Sciences and Purdue University Center for Cancer Research, Purdue University, 915 W State St, West Lafayette IN 47907-1392, USA

Kristen N. Fantetti: kfantett@purdue.edu; Donna M. Fekete: dfekete@purdue.edu

Abstract

Mechanosensory hair cells of the chicken inner ear are innervated by the peripheral processes of statoacoustic ganglion (SAG) neurons. Members of several morphogen families are expressed within and surrounding the chick inner ear during stages of SAG axon outgrowth and pathfinding. Based on their localized expression patterns, we hypothesized that BMPs, FGFs and Shh may function as guidance cues for growing axons and/or may function as trophic factors once axons have reached their targets. To test this hypothesis, three-dimensional collagen cultures were used to grow embryonic day 4 (E4) chick SAG explants for 24 hours in the presence of purified proteins or beads soaked in proteins. The density of neurite outgrowth was quantified to determine effects on neurite outgrowth. Explants displayed enhanced neurite outgrowth when cultured in the presence of purified BMP4, BMP7, a low concentration of Shh, FGF8, FGF10, or FGF19. In contrast, SAG neurons appeared unresponsive to FGF2. Collagen gel cultures were labeled with TUNEL and immunostained with anti-phospho-histone H3 to determine effects on neuron survival and proliferation, respectively. Treatments that increased neurite outgrowth also yielded significantly fewer apoptotic cells, with no effect on cell proliferation. When presented as focal sources, BMP4, Shh, and FGFs -8, -10, and -19 promoted asymmetric outgrowth from the ganglion in the direction of the beads. BMP7-soaked beads did not induce this response. These results suggest that a subset of morphogens enhance both survival and axon outgrowth of otic neurons.

Keywords

BMP; FGF; inner ear; neurotrophic; Shh

Introduction

The avian inner ear contains seven vestibular organs and one auditory organ. Each sensory organ contains mechanosensory hair cells that are innervated by the peripheral processes of statoacoustic ganglion (SAG) neurons. During development, SAG axons are presumed to be guided to their sensory targets by axon guidance cues present along their trajectory (Webber and Raz, 2006; Fekete and Campero, 2007; Appler and Goodrich, 2011) and their survival requires interactions with their targets (Fritzsch, 2003; Yang et al., 2011). Classic axon guidance molecules such as the semaphorins (Gu et al., 2003) and ephrins (Bianchi and Gray, 2002), as well as neurotrophins (Tessarollo et al., 2004; Fritzsch et al., 2005) are

*Corresponding author. Tel.: +1 (765) 496-3058; Fax: +1 (765) 494-0876.

involved. However, members of the bone morphogenetic protein (BMP), sonic hedgehog (Shh), Wnt, and fibroblast growth factor (FGF) families are also expressed within and surrounding the inner ear during stages of SAG axon outgrowth and pathfinding, in both birds (Oh et al., 1996; Wu and Oh, 1996; Farkas et al., 2003; Alsina et al., 2004; Sanchez-Calderon et al., 2004; Bok et al., 2005; Sanchez-Calderon et al., 2007; Chang et al., 2004) and mammals (Morsli et al., 1998; Pirvola et al., 2002; Riccomagno et al., 2002; Pauley et al., 2003; Hayashi et al., 2007; Jacques et al., 2007; Driver et al., 2008; Jahan et al. 2010; Liu et al. 2010; Ohyama et al., 2010). The expression pattern of these molecules makes them candidate chemotropic factors for axons that are navigating towards their sensory targets and candidate chemotrophic factors for axons that have reached their targets.

Morphogens are secreted proteins that exist as concentration gradients and exert concentration dependent effects on target cells at a distance (Charron and Tessier-Lavigne, 2005). They initially participate in tissue patterning during development by specifying cell fate, and then serve as axon guidance cues (Zou and Lyuksyutova, 2007). For example, BMP and Shh are expressed in opposing gradients in the neural tube to specify dorsal and ventral cell fates, respectively. BMP7 is expressed in the roof plate to repel commissural axons ventrally towards the floor plate (Augsburger et al., 1999) and Shh, expressed in the floor plate, attracts commissural axons ventrally (Charron et al., 2003). To date, BMPs are considered repellents, with no reports of them being attractive (Zou and Lyuksyutova, 2007). Shh serves as an attractant in some systems and serves as a repellent in others (Sanchez-Camacho and Bovolenta, 2009). Due to the diverse roles that morphogens play during development, how a particular ligand influences developing neurons appears to be very context and system dependent.

We have recently shown that SAG neurons are unresponsive to Wnts -1, -4, -5a, -6, and -7b *in vitro*, and Wnts -4, and -5a *in vivo* (Fantetti et al., 2011). Therefore, we have focused on testing the responses of SAG neurons to other morphogens that are known to be present during ear development. Several morphogens (BMPs, FGFs, Shh) promoted SAG neuron survival in a collagen gel assay and all except BMP7 promoted SAG neurite outgrowth in a bead assay. The results from this study suggest that SAG neurons may rely on morphogens as survival factors and possible guidance cues, during innervation of the auditory and vestibular systems.

Methods

Explant dissection and culture

Fertilized White Leghorn chicken eggs (Purdue University Farm) were incubated at 38 °C and staged (Hamburger and Hamilton, 1951) prior to dissection. HH20-25 SAG and HH24-25 spinal cord explants were dissected and cultured as described (Bianchi and Cohan, 1993; Fantetti et al., 2011; Fantetti and Fekete, 2011). Explants were cultured in 1.5 mg/ml rat-tail type I collagen (BD Biosciences) gels for 24 hours, under serum-free conditions, supplemented with 10 ng/ml NT-3 (Sigma), 10 ng/ml CNTF (Sigma), and 10% ITS+ (Sigma) to enhance survival. To visualize neuron cell bodies and neurites, explants were fixed and stained with monoclonal anti-β-tubulin (Sigma) as described (Fantetti et al., 2011).

Recombinant proteins were purchased from R&D Systems. Purified human BMP4 (10-100 ng/ml), BMP7 (0.25-1.0 μg/ml), Shh-N (0.5-20 μg/ml), FGF2 (1-20 ng/ml), FGF10 (50-200 ng/ml), FGF19 (50-200ng/ml), and mouse FGF8 (50-500 ng/ml) were diluted in phosphate-buffered saline (PBS) and added to culture medium. PBS was added to control cultures. For inhibitor experiments, 1 μg/ml mouse noggin (R&D Systems), 2 μg/ml mouse follistatin (R&D Systems), 10 μM Cyclopamine (Calbiochem), or 0.1 μM SU5402 (Tocris Bioscience) was added to culture medium.

Beads were prepared for co-cultures as described (Fantetti and Fekete, 2011). Briefly, Affi-gel Blue gel beads (BioRad #153-7302) were soaked for 1-2 hours at room temperature in either PBS (control), 10 μg/ml BMP4, 10 μg/ml BMP7, 2.5 μg/ml Shh-N, or 500 ng/ml FGF -8, -10, -19. Beads were positioned 50-500 μm from the edge of explants prior to collagen polymerization. Standard serum-free culture medium that is used to maintain SAG explants was added to cultures.

Quantitative analysis of neurite outgrowth

Immunostained explant cultures were imaged with a 10× objective on a Nikon C1-plus confocal microscope. Cultured ganglia tend to flatten against the bottom of the culture dish to assume dimensions that are typically 200-400 μm wide by 100-150 μm deep. Furthermore, when imaged from the bottom of the gel, axons projecting vertically into the gel are often too deep to image. Thus, the imaged axons and corresponding measurements are biased in favor of those growing parallel to the bottom of the gels. Image stacks were collapsed into 2D projections and quantified using NIH ImageJ software. Pixel measurements were performed to quantitatively determine neurite responsiveness. For each image, the threshold was adjusted to convert the image into black (neurites) and white (background). The explant was excluded from the image by outlining the explant and cropping the image. The number of pixels occupied by neurites (black) was quantified and normalized to the length of the explant, to control for variation in explant size. SAG neurite length (not shown) and spinal cord neurite outgrowth measurements were performed as described (Fantetti et al., 2011).

For purified protein experiments, effects on neurite outgrowth were determined by quantifying pixels for the entire explant and the explant circumference was used as the length. For bead co-cultures, effects on neurite outgrowth were evaluated by comparing neurite outgrowth facing the bead with outgrowth opposing the bead. Images of co-cultures were divided into 4 quadrants. Neurite outgrowth (in pixels/explant length) for the proximal (facing the bead) and distal (opposing bead) quadrants was quantified. Explant length was measured along the explant edge between the boundaries of the measured quadrant. The pixel ratio of proximal/distal was calculated for each explant. The average of the normalized values was calculated for each treatment group. A ratio equal to 1 was obtained for control cultures and treated cultures with no effect on neurite outgrowth, because there was no difference between the proximal (P) and distal (D) quadrants. A value greater than 1 reflects more neurite outgrowth in the proximal quadrant (neurite promotion) and a value of less than 1 reflects less neurite outgrowth in the proximal quadrant.

Tunel labeling and cell death quantification

After confocal imaging, collagen gels were processed again to evaluate cell death. A similar protocol has been described elsewhere (Fantetti et al., 2011). Gels were incubated overnight in 30% sucrose in PBS, embedded in tissue freezing medium (Triangle Biomedical Sciences), and cryosectioned at 15 μm. Two series of sections were collected to perform TUNEL labeling on alternate sections. To detect apoptotic cells, terminal dUTP nick-end labeling (TUNEL) was performed using a TUNEL kit (In situ Cell Death Detection kit, TMR Red; Roche Applied Science). The manufacturer's protocol was followed with one modification: enzyme and label solutions were diluted 1:1 with TUNEL dilution buffer (Roche Applied Sciences). Sections incubated with dUTP (label solution) alone or DNase I for 10 min prior to TdT were used as negative and positive controls, respectively. Cell nuclei were counter-stained with DRAQ5 (Cell Signaling Technology), diluted 1:1000 in PBS. All sections were imaged with 40x objective on a Nikon-C1 confocal microscope. Manual cell counts were performed from 2D projections of the two middle sections of each explant (Fig 1A-C), using NIH ImageJ software. The percentage of TUNEL-positive cells was calculated

by dividing the number of TUNEL/DRAQ5 double-positive cells by the total number of DRAQ5 labeled cells.

Phospho Histone H3 immunohistochemistry and cell proliferation quantification

Immunostaining was performed on cryosections alternate to sections that were TUNEL labeled. Sections were fixed in 4% paraformaldehyde for 20 minutes at room temperature, rinsed in PBS, and incubated in blocking solution (10% calf serum, 0.1% TX-100, 0.1% sodium azide in PBS) for 1 hour at room temperature. To visualize proliferating cells, sections were incubated for 1 hour at room temperature with rabbit polyclonal PhosphoDetect Anti-Histone H3 (pH3; Calbiochem) diluted 1:200 in blocking solution, rinsed in PBS, and incubated for 1 hour at room temperature with Alexa fluor 568 goat anti-rabbit (Molecular Probes) diluted 1:500 in blocking solution. After PBS rinses, sections were counter-stained with Hoescht33258 (Invitrogen), diluted 1:10000 in PBS, for 10 minutes at room temperature. Sections were rinsed for 5 minutes in PBS and coverslipped with VECTASHIELD HardSet (Vector Laboratories). Sections were imaged with a 20× objective on a Nikon Eclipse E800 microscope and quantified the same day as staining. Manual cell counts were performed from the 3 middle sections (alternate to TUNEL sections) of each explant. The percentage of proliferating cells was calculated by dividing the number of pH3/Hoescht double-positive cells by the total number of Hoescht labeled cells. See Figure 1 for representative staining.

DF-1 survival assay for bioactivity of purified human FGF2

UMNSAH/DF-1 chicken embryo fibroblasts (DF-1 cells; ATCC) were seeded into collagen gels at 6.5×10^5 cells per well and cultured for 24 hours with SAG culture medium supplemented with PBS (control) or 1-10 ng/ml FGF2. Gels were immunostained as described for explant cultures (Fantetti et al., 2011). Apoptotic cells were labeled with rabbit polyclonal anti-caspase 3 (R&D Systems) and all cells were counterstained with DRAQ5 (Cell Signaling Technology). Images were taken with a confocal microscope and collapsed into 2D projections. The number of apoptotic cells (caspase3/DRAQ5 double-positive) and DRAQ5-positive cells were manually counted and the percentage of apoptotic cells was calculated by dividing the number of double-positive cells by the total number of cells.

Statistical Analysis

Measurements are given in mean ± standard error (SE). Means represent data collected from 2-3 independent experiments for each condition. To determine statistically significant effects, a one-way ANOVA (followed by a Tukey's multiple comparisons test) or a student's t-test was performed using GraphPad Software (GraphPad Software Inc). Results were considered statistically significant with a p value of less than 0.05.

Results

BMP4 promotes SAG neurite outgrowth and neuron survival

Bmp4 transcripts are expressed by prosensory regions of the inner ear (Fig. 2A; Wu and Oh, 1996) that will become innervated, suggesting that SAG neurons may be BMP4-responsive. After 24 hours in culture, SAG explants displayed longer and denser neurite outgrowth in the presence of BMP4 (Fig. 2C) compared to controls (Fig. 2B). Image analysis revealed that 10-100 ng/ml BMP4 treatment produced average pixel numbers that were significantly greater than controls (Fig. 2H; ANOVA, $p<0.0001$). Noggin inhibits BMP signaling by binding with high affinity to BMP4 ligands (Zimmerman et al., 1996). When explants were cultured in the presence of Noggin alone or Noggin and BMP4, neurite outgrowth resembled

controls (Fig. 2E, F, H). These results suggested that BMP4 promotes SAG neurite outgrowth.

An enhancement of neurite outgrowth could result from increased cell numbers due to trophic effects on proliferation or survival rather than, or in addition to, any neurotropic effects. To evaluate effects on cell survival, TUNEL assays were performed to detect apoptotic cells with double-stranded DNA breaks (Gavrieli et al., 1992). If BMP4 promoted SAG neuron survival, we expected there to be fewer TUNEL positive cells for BMP4-treated explants than for untreated explants. There were significantly fewer TUNEL positive neurons in the presence of 50 ng/ml BMP4 compared to controls (Fig. 2I; t-test, $p<0.0001$). Proliferating cells were immunolabeled with anti-phospho-histone H3 (pH3). Under these culture conditions, most SAG neurons are postmitotic on E4-5, as shown by very low percentages of pH3/Hoescht double-positive cells. BMP4 did not affect cell proliferation (Fig. 2J; t-test, $p=0.4928$). From these results we concluded that BMP4 promotes the survival of SAG neurons under these culture conditions.

Bath application of proteins does not create a morphogen point source, which is necessary to assay for directional effects on neurites. Placing a bead at a distance may permit proteins to diffuse from the beads and may create a protein gradient through the collagen gel. To test the possibility that BMP4 may serve as a directional cue for growing neurites, in addition to promoting neuron survival, we tested the responses of SAG neurites to a point source of BMP4. Beads were incubated in PBS (Fig. 2D; Control) or 10 μg/ml BMP4 (Fig. 2G) and placed into collagen gels so that they were usually a few hundred microns from the explant edge. If BMP4 was neurite promoting or attractive, we expected neurites to preferentially grow towards a BMP4-soaked bead. After 24 hours in culture, SAG neurites were short and did not orient towards or away from control-treated beads (Fig. 2D). On the other hand, neurites were denser and longer in the presence of BMP4-treated beads and displayed more robust outgrowth on the side of the explant facing the bead (Fig. 2G). Quantitatively, there was significantly greater neurite outgrowth in the proximal (facing the bead) quadrant compared to the distal (opposite) quadrant (Fig. 2K; ANOVA, $p<0.0001$). From these results we concluded that BMP4 promotes SAG neuron survival and neurite outgrowth under these culture conditions.

BMP7 promotes SAG neuron survival

On E4, Bmp7 is broadly expressed within the ventral otocyst, including the mesenchyme, and overlaps with Bmp4 expression in the prosensory domains (Fig. 3A; Oh et al., 1996). SAG explants cultured for 24 hours displayed significantly greater neurite outgrowth in the presence of BMP7 compared to controls (Fig. 3B, C, J; ANOVA, $p<0.0001$). Follistatin inhibits BMP7 function by binding with high affinity to BMP7 ligands (Lemura et al., 1998). When explants were cultured in the presence of Follistatin alone or Follistatin and BMP7, there was no significant difference in outgrowth compared to controls (Fig. 3F, G, J), suggesting that the effects we observed were due to the addition of BMP7. Furthermore, there was a 3-fold reduction in the percentage of TUNEL positive neurons in the presence of 0.5 μg/ml BMP7 compared to controls (Fig. 3K; t-test, $p<0.0001$), with no change in the mitotic index (Fig. 3L; t-test, $p=0.2668$).

BMP7 was also expected to promote outgrowth as a point source, after observing enhanced neurite outgrowth in the presence of purified BMP7. However, SAG neurites appeared unresponsive to beads soaked in 10 μg/ml BMP7 (Fig. 3D, H). There was no significant difference in outgrowth between control and BMP7-treated cultures (Fig. 3M; ANOVA, $p=0.5441$) and neurites did not orient towards or away from BMP7 beads (Fig. 3D, H). Before accepting these negative data, positive control tissues, known to be BMP7-responsive, were used to confirm bioactivity of the BMP7-treated beads. In the mouse,

BMP7 repels neurite outgrowth from mouse dorsal spinal cord explants *in vitro* (Augsburger et al., 1999). The current study replicated the outgrowth inhibiting effects of BMP7 seen in the mouse by culturing E4 chick dorsal spinal cord explants under the same conditions as E4 SAG explants, on the same day. We observed reduced neurite outgrowth from BMP7-treated explants compared to controls (Fig. 3E, I). Quantification of neurite outgrowth showed significantly less outgrowth in pixels per unit length (ANOVA, $p<0.0001$) for explants cultured with beads soaked in 1 μg/ml (10.74 ± 1.03, n=10) and 10 μg/ml BMP7 (3.26 ± 1.16, n=7) compared to controls (23.63 ± 1.78, n=10). This confirmed that the beads soaked in purified BMP7 were bioactive, thus strengthening the conclusion that BMP7 does not influence SAG neurite outgrowth.

Responses to Shh are concentration-dependent

Notochord and floorplate sources of Shh are known to directly influence ear development in the chick (Bok et al., 2005). We hypothesized that a ventral source of Shh may attract a subset of SAG neurites to grow ventrally, towards the cochlear duct, or may repel neurites to prevent them from projecting too far ventrally (past the cochlear duct). To test this hypothesis, responsiveness to 0.5-20 μg/ml of Shh was tested and we observed concentration-dependent responses (Fig. 4). The lowest Shh concentration, 0.5 μg/ml, produced significantly greater neurite outgrowth compared to controls (Fig. 4A, B, I; ANOVA, $p<0.0001$). Cyclopamine specifically inhibits Shh signaling by binding to smoothened, the transmembrane protein required for pathway activation (Chen et al., 2002; Frank-Kamenetsky et al., 2002; Incardona et al., 1998). Adding Cyclopamine to culture medium abrogated the neurite-promoting effects of Shh (Fig. 4E, F, I), as expected if Shh exerts a direct effect. We also observed significantly fewer TUNEL positive neurons in the presence of 0.5 μg/ml Shh (Fig. 4J; ANOVA, $p<0.0001$).

In contrast, higher concentrations of Shh, in the range of 5-20 μg/ml, inhibited neurite outgrowth. Explants displayed significantly fewer and shorter neurites compared to controls (Fig 4A, C, I; ANOVA, $p<0.0001$). Interestingly, the amount of neurite outgrowth at 5 μg/ml is not significantly different from that observed at 10 and 20 μg/ml (Fig. 4I). As well, cyclopamine did not rescue the reduction in neurite outgrowth seen at 5 μg/ml Shh (Fig. 4I). This suggested that high Shh concentrations may inhibit neurite outgrowth without binding to smoothened, possibly acting as a toxin. TUNEL assays were performed to determine if Shh addition was associated with higher levels of cell death. The percentage of TUNEL positive neurons increased with Shh concentration, but only the 20 μg/ml concentration reached a statistically significant difference from untreated controls (Fig. 4J; ANOVA, $p<0.0001$). Overall, it appears that Shh becomes increasingly toxic to SAG neurons at high concentrations and this may explain the reductions in neurite outgrowth (Fig. 4I).

Less than 1 percent of SAG neurons were positively labeled with pH3 when fixed after 24h in culture. There was no significant difference in the mitotic index between control and Shh-treated cultures (Fig. 4K; ANOVA, $p=0.4500$). Therefore, we expected that the effects on neurite outgrowth and neuron survival were not due to differences in the proportion of proliferating cells between treatment groups.

Explants were also co-cultured with beads that were incubated in either PBS (Control; Fig. 4D) or 2.5 μg/ml Shh (Fig. 4H). Both neurite promoting and inhibiting responses were considered based on the concentration-dependent responses obtained with purified proteins (Fig. 4A-C, I). Significantly denser and longer neurite outgrowth was observed for neurites facing Shh-coated beads compared to the side of the explant opposing the bead (Fig. 3H) and compared to neurites facing control beads (Fig. 4D, L; t-test, $p<0.05$). Beads were also incubated in higher concentrations of Shh (5, 10, 20, 40 μg/ml) to assay for a repulsive response, but neurite outgrowth resembled that observed for the 2.5 μg/ml condition (not

shown). This suggested that either Shh is not repulsive to SAG neurites or that the beads are already saturated with proteins when incubated in 2.5 μg/ml Shh, and incubating beads in higher concentrations of Shh does not increase the amount released by the bead. To create a larger Shh point source, irrespective of the amount of protein on the beads, several Shh beads were placed adjacent to the explant. A repulsive response was still not observed (not shown), suggesting that in combination with the TUNEL results, high Shh concentrations are toxic to SAG neurons, which results in reduced neuron survival and reduced neurite outgrowth.

FGF8, FGF10, and FGF19 promote SAG neuron survival and neurite outgrowth

FGF8 (Fig. 5), FGF10 (Fig. 6), and FGF19 (Fig. 7) also produced concentration- dependent neurite outgrowth responses. FGF8 and FGF19 significantly promoted neurite outgrowth at 50, 100, and 200 ng/ml, but at 500 ng/ml neurite outgrowth was comparable to control levels (Fig. 5H, 7H; ANOVA, $p<0.0001$). Only the 200 ng/ml FGF10 concentration significantly promoted SAG neurite outgrowth (Fig. 6B, C, H, ANOVA; $p<0.01$). SU5402 is a tyrosine kinase activity inhibitor that inhibits FGF receptor activation (Mohammadi et al., 1997), thus interfering with FGF signaling. SU5402 abrogated the neurite-promoting effects of FGF8 (Fig. 5E, F, H) and FGF19 (Fig. 7E, F, H), but not FGF10 (Fig. 6E, F, H). The increase in neurite outgrowth in cultures with FGFs was associated with a reduction in the percentage of TUNEL-positive neurons. FGF10- and FGF19-treated SAGs showed a 2-fold reduction in the percentage of TUNEL positive cells compared to controls (Fig. 6I, t-test, $p<0.01$; 7I, $p<.0001$), whereas FGF8 had a weaker effect (Fig. 5I; ANOVA, $p<0.01$). Neither FGF8 (Fig. 5J; ANOVA, $p=0.1742$), FGF10 (Fig. 6J; t-test, $p=0.8366$), nor FGF19 (Fig. 7J; t-test, $p=0.8706$) affected the mitotic index when compared to controls.

Fgf8 is expressed in the sensory patches of the saccule and lagena (vestibular organs), but is absent from the auditory sensory region, the basilar papilla (Sanchez-Calderon et al., 2004). Fgf19 is strongly expressed in the sensory regions of the utricle and lagena (vestibular organs), the SAG neurons, and some of the prosensory region borders, but is also absent from the auditory basilar papilla (Sanchez-Calderon et al., 2007). Based on these expression patterns, we hypothesized that FGF8 and FGF19 may be important for guiding subsets of vestibular axons or for repelling auditory axons from innervating vestibular sensory regions during development. Explants were cultured with beads that were treated with PBS, FGF8 or FGF19. Effects on overall outgrowth (promotion and inhibition) as well as directional outgrowth towards (attraction) or away from (repulsion) the bead were all considered. FGF8-treated beads (Fig. 5D, G) and FGF19-treated beads (Fig. 7D, G) both promoted neurite outgrowth. At this developmental stage, the SAG contains vestibular and auditory neurons that will soon separate into two ganglia, so the neurites are probably somewhat segregated within the explants. If only a subset of neurites was responding to the bead, we expected there to be an asymmetric neurite outgrowth pattern in the purified protein cultures, but this pattern was not observed (Fig. 5B, C; 7B, C). Quantitatively, there was significantly greater neurite outgrowth on the side of the explants that were facing beads soaked in FGF8 (Fig. 5K; t-test, $p<0.01$) or FGF19 (Fig. 7K; t-test, $p<0.0001$). In the mouse, Fgf10 is expressed by all sensory organs and SAG neurons (Pirvola et al., 2000). However, there is limited FGF10 expression data for the chick. At HH26, FGF10 has been shown to be strongly expressed in the anterior and lateral cristae and the utricular macula, weakly expressed by the posterior crista (Fig. 6A; Chang et al., 2004) and absent from SAG neurons on E2-3 (Alsina et al., 2004). To test the hypothesis that FGF10 may exert directional effects on neurite outgrowth, in addition to promoting neuron survival (Fig. 6I), we cultured explants with beads that were soaked in PBS (Fig. 6D) or 500 ng/ml FGF10 (Fig. 6G). We observed significantly greater neurite outgrowth in the presence of FGF10-treated beads compared to control cultures (Fig. 6K; t-test, $p<0.01$). These results suggest that in addition

to providing trophic support for SAG neurons, FGFs -8, -19, and -10 may also provide outgrowth promoting cues for growing SAG neurites.

E4 SAG neurons are unresponsive to purified FGF2

FGF2 was tested because it promotes the survival of early (E2-3) and late (E8-16) stage chick SAG neurons *in vitro* (Hossain et al., 1996; Carnicero et al., 2001). We found no significant difference in neurite outgrowth between control and FGF2-treated explants (Fig. 8A; ANOVA, $p=0.7874$). Bioactivity of FGF2 was confirmed by performing a cell survival assay under the same culture conditions that were used for SAG explants. DF-1 chicken embryo fibroblasts were cultured in collagen gels for 24 hours with or without FGF2. Apoptotic cells were stained with anti-caspase3 and all cell nuclei were stained with DRAQ5. There were significantly fewer caspase3-positive cells in the presence of FGF2 compared to controls (Fig. 8B; ANOVA, $p<0.0001$). From these results we concluded that FGF2 promotes DF-1 survival and is bioactive under SAG explant culture conditions.

Combinations of purified proteins do not produce additive effects

The expression patterns of some of the morphogens we tested either overlap or are mutually exclusive of one another. For example, the spatial distribution of Bmp4 and Bmp7 transcripts are largely similar (Fig. 2A, 3A), whereas Fgf8 and Fgf19 transcripts are mostly non-overlapping (Fig. 5A, 7A). If subpopulations of neurites are differentially responsive to single proteins added to culture medium, it might be possible to detect additive effects on neurite outgrowth with combinations of proteins. We tested the effects of BMP4+7, BMP4+FGF8, and FGF8+19. In each case, neurite outgrowth was comparable to what was observed when one protein was added to the cultures (not shown). These results led us to conclude that additive effects, if present, must be insufficiently robust to detect with the quantification methods used here.

Discussion

Morphogens are expressed within and surrounding the inner ear during stages of SAG neurite outgrowth and sensory organ innervation. Based on published expression data, we hypothesized that some morphogens may be important for guiding SAG axons towards their sensory targets and/or may be important for promoting SAG neuron survival. In an earlier study, we reported that E4 SAG neurites were unresponsive to some members of the Wnt morphogen family (Fantetti et al., 2011). In this study, we have expanded the Wnt results by testing the responsiveness of SAG neurons to some members of the BMP, Shh, and FGF morphogen families. Experiments were carried out *in vitro* to determine SAG responsiveness to individual molecules, to avoid potential confounding variables in a complex *in vivo* environment. We provide evidence that some of the molecules that we tested enhance survival and promote neurite outgrowth of SAG neurons.

During development, a single morphogen can regulate neurogenesis, neuron survival, and axon guidance in the same tissue. For example, during spinal cord development, Shh first regulates neurogenesis and cell survival, and then is used as a chemotropic cue to guide commissural axons ventrally (Chiang et al., 1996; Briscoe and Ericson, 1999; Jessell, 2000; Litingtung and Chiang, 2000; Charron et al., 2003). As a result, Shh is both a trophic (promotes cell survival) and a tropic (directs axon outgrowth) factor. Under culture conditions, neuronal survival will reflect a balance between cell proliferation (neurogenesis) and cell death, and both were evaluated in the current study of SAG neurons. Assuming a relatively uniform responsiveness among the population of treated cells, more neurons would be expected to make more neurites. Indeed, SAG explants with enhanced neurite outgrowth contained significantly fewer TUNEL positive cells, suggesting improved neuron

survival. But there was no additional effect of morphogen treatment on neurogenesis. An isolated E4 chicken SAG should contain both progenitors and neurons: the first SAG neurons begin to differentiate on E3 and are all postmitotic by E7 (D'Amico-Martel, 1982). In fact, overall neurogenesis was rather modest in control cultures (with added CNTF and NT-3), as reflected by a mitotic index of approximately 1%. There was no change in this mitotic index among cultures grown in the presence of purified morphogens, suggesting that neurogenesis was relatively constant across conditions. We confirmed that the proliferation assay we employed (phospho-histone-H3 immunostaining) was sensitive enough to detect a significant change (2-fold) in the mitotic index. Specifically, SAGs grown in serum-free conditions and only supplemented with 20 or 100 ng/ml of insulin-like-growth factor-1 (IGF-1) had elevated mitotic indices as compared to untreated explants (i.e., those grown in serum-free media without additional supplements; data not shown). A similar response to IGF-1 was reported previously for E3 SAGs cultured either in isolation or in association with the otocyst: neurons displayed enhanced neurite outgrowth and increased cell proliferation when treated for 24 hours with IGF-1 (Camarero et al., 2003). In summary, morphogen treatments that stimulated SAG neurite outgrowth may have done so by enhancing neuron survival, but apparently not by increasing neurogenesis.

In addition to the aforementioned trophic effects, we sought to address the question of whether enhanced neurite outgrowth was also induced by direct tropic effects on the neurites. This was examined by asking whether focal sources of morphogens could promote local outgrowth from the ganglion or turn the neurites towards the beads. Only BMP7 lacked the ability to promote neurite outgrowth on the side of the explant facing the beads. This led us to consider the degree to which differences in neuron survival could account for differing outgrowth responses. BMP7-treated cultures had the largest (3-fold) reduction in the percentage of TUNEL-positive neurons and Bmp7 transcripts display the broadest expression pattern across sensory and non-sensory regions (Oh et al., 1996). For BMP7, we presume that increases in neurite outgrowth are more likely to be explained by enhanced neuron survival than by directional outgrowth. Alternatively, FGF8 produced the weakest reduction in the proportion of TUNEL-positive neurons, but when presented as a point source significantly promoted neurite outgrowth. It is possible that for FGF8, enhanced neurite outgrowth is more accounted for by neurite responsiveness than it is by neuron survival. It appears that some of the molecules we tested may be more important for survival than they are for promoting outgrowth. Neurite length measurements (not shown) were performed for purified protein studies and produced similar results and statistical significance as pixel measurements. Similarly, bead co-cultures with an increase in outgrowth density also displayed longer neurites. Therefore, it is also possible that enhanced neurite outgrowth may have been due to changes in axon properties that we did not quantify, such as outgrowth rate, as observed for BMP chemorepellents and spinal cord commissural axons (Phan et al., 2010).

Studies from mammalian and zebrafish systems suggest that our results with BMP4, Shh, and FGF10 may extend to other species. In the postnatal mouse, BMP4 promotes dissociated spiral ganglion neuron survival *in vitro* (Whitlon et al., 2007) and cultures of dissociated rat spiral ganglion neurons show enhanced survival when co-cultured with olfactory ensheathing cells that are known to express BMP4 (Liu et al., 2010). Additionally, *Bmp4* mutant mice display reduced cochlear innervation (Blauwkamp et al., 2007), suggesting that BMP4 may be important for survival or axon guidance *in vivo*. Deletion of Shh in the inner ear blocks the appearance of the cochlea, saccule, and spiral ganglion in mice (Riccomagno et al., 2005; Brown and Epstein, 2011). Similarly, loss of Hedgehog signaling in zebrafish results in reduced posterior macula innervation and a reduced SAG (Sapede and Pujades, 2010). In these studies, the absence of Shh signaling may directly prevent neuronal specification. However, neuronal loss may also be secondary to the loss of sensory

structures and the trophic support that they provide. FGF10 is expressed by spiral ganglion neurons and sensory epithelia (Pirvola et al., 2000) in the mouse, and may be important for neuron survival (Wright and Mansour, 2003). *Fgf10*$^{-/-}$ mice lack a posterior crista (Pauley et al., 2003) and show an increase in the proportion of apoptotic neurons (Pirvola et al. 2000). The number of fibers contacting vestibular sensory epithelia is also reduced (Pirvola et al., 2000; Pauley et al., 2003). These results suggest that FGF10 is an important trophic factor *in vivo* for the mouse. Our results support the possibility that BMPs, Shh and FGFs may serve as trophic factors once neurons begin to differentiate, not only in the chicken but also perhaps in other species.

On the other hand, expression data and results from functional studies suggest that some of the molecules we tested may have different functions on SAG neurons in different species. While Bmp4 is expressed in all prosensory regions in the chick (Wu and Oh, 1996), in the mouse it is restricted to the prosensory cristae (Morsli et al., 1998) and is not present in the auditory prosensory region (Ohyama et al., 2010). It is possible that in the mouse, BMP4 in vestibular prosensory regions serves as a chemoattractant and that BMP4 in non-sensory regions of the cochlea serves as a chemorepellent or has no effect. Shh is not expressed in the otocyst of the mouse (Riccomagno et al., 2002) nor the chick (Bok et al., 2005), but is expressed by mouse spiral ganglion neurons between E13.5 and P0 (Driver et al., 2008; Liu et al., 2010). To date, Shh expression has not been described for the chick SAG. The differences in Shh sources may result in differing responses of otic neurons to Shh across systems. FGF2 increases the survival of E2-3 chick SAG (Hossain et al., 1996) and E10.5-12 mouse spiral ganglion (Hossain and Morest, 2000) *in vitro*. In contrast, we found E4 SAG neurons to be unresponsive to FGF2. The time-sensitive responses of chick SAG to FGF2 (Carnicero et al., 2001; Hossain et al., 2002) likely account for the lack of a response in the current study. Fgf8 is expressed in the sensory patches of the saccule and lagena (vestibular organs), but is absent from the auditory sensory region of the chick (Sanchez-Calderon et al., 2004). In the mouse, FGF8 is expressed in the inner hair cells of the cochlea (auditory organ; Hayashi et al., 2007; Jacques et al., 2007). Therefore, vestibular and auditory neurons may be differentially responsive to FGF8 in the chick and mouse, respectively. In the current study, FGF10 promoted SAG neurite outgrowth and neuron survival, but SU5402 failed to inhibit these effects. Thus, FGF10 may indirectly activate other signaling pathways in this system.

Although morphogen combination experiments yielded no additive effects on neurite outgrowth, we cannot exclude the possibility that combining neurotrophins (specifically CNTF and NT-3) with morphogens in our culture system altered the responsivity of SAG neurons. For example, BMP4 reduces the number of mouse sympathetic neurons *in vitro*, but when combined with NGF, the effects are reversed (Gomes and Kessler, 2001). In this system, BMP4 increases the dependence on neurotrophins (Gomes and Kessler, 2001). In another example, when mouse spiral ganglion neurons are cultured with FGF2, in combination with NT-3 or BDNF, neuroblast migration and neurite outgrowth are enhanced beyond levels of that observed with FGF2 alone (Hossain et al., 2008). It is possible that some of the morphogens we tested altered the dependence of SAG neurons on CNTF or NT-3 and thus acted indirectly on neuronal survival.

An *in vitro* approach provides a controlled and simplified environment to evaluate neurite outgrowth responses to individual molecules. This offers an alternative to *in vivo* gain- and loss-of-function approaches, where patterning defects can severely disrupt ear development and indirectly cause innervation defects as discussed earlier. However, there are limitations to using an *in vitro* system in the way that we have presented it here. First, on E4 the SAG consists of a heterogeneous cell population. There are two populations of neurons (vestibular and auditory), two populations of axons (peripheral and central), and non-neuronal cells (eg.

glial, endothelial). Subpopulations of neurons and axons may be differentially responsive. For example, cultures of dissociated mouse spiral ganglion neurons contain more monopolar neurons in the presence of BMP4 (Whitlon et al., 2007), suggesting that central and peripheral processes may respond differently to BMP4. Due to the technical limitations of our *in vitro* system, we were unable to distinguish between these cell and neurite populations. Furthermore, non-neuronal cell types present in our cultures can serve as a target for the applied molecules. Schwann cells express neurotrophins that promote spiral ganglion neuron survival and consequently spiral ganglion neurites preferentially grow on Schwann cells *in vitro* (Hansen et al., 2001); Bostrom et al., 2009; Whitlon et al., 2009; Jeon et al., 2011). If morphogens influence Schwann cell development or survival, this could indirectly contribute to the responses we observed.

In summary, is the first study to directly test the responses of E4 chick SAG neurons to members of the BMP, Shh, and FGF morphogen familes. Our results suggest that morphogens, in addition to classic axon guidance molecules and neurotrophins, are also capable of regulating sensory neuron survival and sensory organ innervation. We provide evidence for how individual molecules regulate SAG neuron survival and neurite outgrowth, but leave open the possibility that there may be different responses to these molecules *in vivo*. Because these morphogen gene families play multiple roles in otic development (Groves and Fekete, 2011), it may be necessary to design targeted, conditional gene knockouts to evaluate their ability to serve as axon guidance cues in intact animals.

Acknowledgments

We thank Doris Wu and Wiese Chang for advice with experiments and Rodney McPhail for help with figure illustrations. This work was funded by the National Institutes of Health Grant RO1DC002756 and the Purdue Research Foundation.

References

Alsina B, Abello G, Ulloa E, Henrique D, Pujades C, Giraldez F. FGF signaling is required for determination of otic neuroblasts in the chick embryo. Dev Biol. 2004; 267:119–134. [PubMed: 14975721]

Appler JM, Goodrich LV. Connecting the ear to the brain: Molecular mechanisms of auditory circuit assembly. Prog Neurobiol. 93:488–508. [PubMed: 21232575]

Augsburger A, Schuchardt A, Hoskins S, Dodd J, Butler S. BMPs as mediators of roof plate repulsion of commissural neurons. Neuron. 1999; 24:127–141. [PubMed: 10677032]

Bianchi LM, Cohan CS. Effects of the neurotrophins and CNTF on developing statoacoustic neurons: comparison with an otocyst-derived factor. Dev Biol. 1993; 159:353–365. [PubMed: 8365572]

Bianchi LM, Gray NA. EphB receptors influence growth of ephrin-B1-positive statoacoustic nerve fibers. European Journal of Neuroscience. 2002; 16:1499–1506. [PubMed: 12405963]

Blauwkamp MN, Beyer LA, Kabara L, Takemura K, Buck T, King WM, Dolan DF, Barald KF, Raphael Y, Koenig RJ. The role of bone morphogenetic protein 4 in inner ear development and function. Hear Res. 2007; 225:71–79. [PubMed: 17275231]

Bok J, Bronner-Fraser M, Wu DK. Role of the hindbrain in dorsoventral but not anteroposterior axial specification of the inner ear. Development. 2005; 132:2115–2124. [PubMed: 15788455]

Bostrom M, Khalifa S, Bostrom H, Liu W, Friberg U, Rask-Andersen H. Effects of neurotrophic factors on growth and glial cell alignment of cultured adult spiral ganglion cells. Audiol Neurootol. 2009; 15:175–186. [PubMed: 19851064]

Briscoe J, Ericson J. The specification of neuronal identity by graded Sonic Hedgehog signalling. Seminars in Cell and Developmental Biology. 1999; 10:353–362. [PubMed: 10441550]

Brown AS, Epstein DJ. Otic ablation of smoothened reveals direct and indirect requirements for Hedgehog signaling in inner ear development. Development. 2011; 138:0000–0000.10.1242/dev.066126

Camarero G, Leon Y, Gorospe I, De Pablo F, Alsina B, Giraldez F, Varela-Nieto I. Insulin-like growth factor 1 is required for survival of transit-amplifying neuroblasts and differentiation of otic neurons. Developmental Biology. 2003; 262:242–253. [PubMed: 14550788]

Carnicero E, Garrido JJ, Alonso MT, Schimmang T. Roles of fibroblast growth factor 2 during innervation of the avian inner ear. J Neurochem. 2001; 77:786–795. [PubMed: 11331407]

Chang W, Brigande JV, Fekete DM, Wu DK. The development of semicircular canals in the inner ear: role of FGFs in sensory cristae. Development. 2004; 131:4201–4211. [PubMed: 15280215]

Charron F, Stein E, Jeong J, McMahon AP, Tessier-Lavigne M. The morphogen sonic hedgehog is an axonal chemoattractant that collaborates with netrin-1 in midline axon guidance. Cell. 2003; 113:11–23. [PubMed: 12679031]

Charron F, Tessier-Lavigne M. Novel brain wiring functions for classical morphogens: a role as graded positional cues in axon guidance. Development. 2005; 132:2251–2262. [PubMed: 15857918]

Chen JK, Taipale J, Cooper MK, Beachy PA. Inhibition of Hedgehog signaling by direct binding of cyclopamine to Smoothened. Genes Dev. 2002; 16:2743–2748. [PubMed: 12414725]

Chiang C, Litingtung Y, Lee E, Young KE, Corden JL, Westphal H, Beachy PA. Cyclopia and defective axial patterning in mice lacking Sonic hedgehog gene function. Nature. 1996; 383:407–413. [PubMed: 8837770]

D'Amico-Martel A. Temporal patterns of neurogenesis in avian cranial sensory and autonomic ganglia. American Journal of Anatomy. 1982; 163:351–372. [PubMed: 7091019]

Driver EC, Pryor SP, Hill P, Turner J, Ruther U, Biesecker LG, Griffith AJ, Kelley MW. Hedgehog signaling regulates sensory cell formation and auditory function in mice and humans. J Neurosci. 2008; 28:7350–7358. [PubMed: 18632939]

Fantetti KN, Zou Y, Fekete DM. Wnts and Wnt inhibitors do not influence axon outgrowth from chicken statoacoustic ganglion neurons. Hear Res. 2011; 278:86–95. [PubMed: 21530628]

Fantetti KN, Fekete DM. Dissection and culture of chick statoacoustic ganglion and spinal cord explants in collagen gels for neurite outgrowth assays. J Vis Exp In Press.

Farkas LM, Dunker N, Roussa E, Unsicker K, Krieglstein K. Transforming growth factor-beta(s) are essential for the development of midbrain dopaminergic neurons in vitro and in vivo. J Neurosci. 2003; 23:5178–5186. [PubMed: 12832542]

Fekete DM, Campero AM. Axon guidance in the inner ear. Int J Dev Biol. 2007; 51:549–556. [PubMed: 17891716]

Frank-Kamenetsky M, Zhang XM, Bottega S, Guicherit O, Wichterle H, Dudek H, Bumcrot D, Wang FY, Jones S, Shulok J, Rubin LL, Porter JA. Small-molecule modulators of Hedgehog signaling: identification and characterization of Smoothened agonists and antagonists. J Biol. 2002; 1:10. [PubMed: 12437772]

Fritzsch B. Development of inner ear afferent connections: forming primary neurons and connecting them to the developing sensory epithelia. Brain Res Bull. 2003; 60:423–433. [PubMed: 12787865]

Fritzsch B, Pauley S, Matei V, Katz DM, Xiang M, Tessarollo L. Mutant mice reveal the molecular and cellular basis for specific sensory connections to inner ear epithelia and primary nuclei of the brain. Hear Res. 2005; 206:52–63. [PubMed: 16080998]

Gavrieli Y, Sherman Y, Ben-Sasson A. Identification of programmed cell death in situ via specific labeling of nuclear DNA fragmentation. Journal of Cell Biology. 1992; 119:493–501. [PubMed: 1400587]

Gomes WA, Kessler JA. Msx-2 and p21 mediate the pro-apoptotic but not the anti-proliferative effects of BMP4 on cultured sympathetic neuroblasts. Dev Biol. 2001; 237:212–221. [PubMed: 11518517]

Groves AK, Fekete DM. Shaping sound in space: the regulation of inner ear morphogenesis by signaling gradients. Development. 2011 manuscript in review.

Gu C, Rodriguez ER, Reimert DV, Shu T, Fritzsch B, Richards LJ, Kolodkin AL, Ginty DD. Neuropilin-1 conveys semaphorin and VEGF signaling during neural and cardiovascular development. Dev Cell. 2003; 5:45–57. [PubMed: 12852851]

Hamburger V, Hamilton HL. A series of normal stages in the development of the chick embryo. Journal of Morphology. 1951; 88:49–91.

Hansen MR, Zha XM, Bok J, Green SH. Multiple distinct signal pathways, including an autocrine neurotrophic mechanism, contribute to the survival-promoting effect of depolarization on spiral ganglion neurons in vitro. J Neurosci. 2001; 21:2256–2267. [PubMed: 11264301]

Hayashi T, Cunningham D, Bermingham-McDonogh O. Loss of Fgfr3 leads to excess hair cell development in the mouse organ of Corti. Dev Dyn. 2007; 236:525–533. [PubMed: 17117437]

Hossain WA, Brumwell CL, Morest DK. Sequential interactions of fibroblast growth factor-2, brain-derived neurotrophic factor, neurotrophin-3, and their receptors define critical periods in the development of cochlear ganglion cells. Exp Neurol. 2002; 175:138–151. [PubMed: 12009766]

Hossain WA, D'Sa C, Morest DK. Interactive roles of fibroblast growth factor 2 and neurotrophin 3 in the sequence of migration, process outgrowth, and axonal differentiation of mouse cochlear ganglion cells. J Neurosci Res. 2008; 86:2376–2391. [PubMed: 18438927]

Hossain WA, Morest DK. Fibroblast growth factors (FGF-1, FGF-2) promote migration and neurite growth of mouse cochlear ganglion cells in vitro: immunohistochemistry and antibody perturbation. Journal of Neuroscience Research. 2000; 62:40–55. [PubMed: 11002286]

Hossain WA, Zhou X, Rutledge A, Baier C, Morest DK. Basic fibroblast growth factor affects neuronal migration and differentiation in normotypic cell cultures from the cochleovestibular ganglion of the chick embryo. Experimental Neurology. 1996; 138:121–143. [PubMed: 8593888]

Lemura S, Yamamoto TS, Takagi C, Uchiyama H, Natsume T, Shimasaki S, Sugino H, Ueno N. Direct binding of follistatin to a complex of bone-morphogenetic protein and its receptor inhibits ventral and epidermal cell fates in early Xenopus embryo. Proc Natl Acad Sci U S A. 1998; 95:9337–9342. [PubMed: 9689081]

Incardona JP, Gaffield W, Kapur RP, Roelink H. The teratogenic Veratrum alkaloid cyclopamine inhibits sonic hedgehog signal transduction. Development. 1998; 125:3553–3562. [PubMed: 9716521]

Jacques BE, Montcouquiol ME, Layman EM, Lewandoski M, Kelley MW. Fgf8 induces pillar cell fate and regulates cellular patterning in the mammalian cochlea. Development. 2007; 134:3021–3029. [PubMed: 17634195]

Jahan I, Pan N, Kersigo J, Fritzsch B. Neurod1 suppresses hair cell differentiation in ear ganglia and regulates hair cell subtype development in the cochlea. PLoS One. 2010; 5:e11661. [PubMed: 20661473]

Jeon EJ, Xu N, Xu L, Hansen MR. Influence of central glia on spiral ganglion neuron neurite growth. Neuroscience. 2011; 177:321–334. [PubMed: 21241783]

Jessell TM. Neuronal specification in the spinal cord: inductive signals and transcriptional codes. Nat Rev Genet. 2000; 1:20–29. [PubMed: 11262869]

Litingtung Y, Chiang C. Control of Shh activity and signaling in the neural tube. Developmental Dynamics. 2000; 219:143–154. [PubMed: 11002335]

Liu Q, Yu HM, Dai CF, Li W, Zhu YY, Gu YR, Li HW. Olfactory ensheathing cells promote the survival of newborn rat spiral ganglion cells in vitro. Sheng Li Xue Bao. 2010; 62:115–121. [PubMed: 20401445]

Liu Z, Owen T, Zhang L, Zuo J. Dynamic expression pattern of Sonic hedgehog in developing cochlear spiral ganglion neurons. Dev Dyn. 2010; 239:1674–1683. [PubMed: 20503364]

Mohammadi M, McMahon G, Sun L, Tang C, Hirth P, Yeh BK, Hubbard SR, Schlessinger J. Structures of the tyrosine kinase domain of fibroblast growth factor receptor in complex with inhibitors. Science. 1997; 276:955–960. [PubMed: 9139660]

Morsli H, Choo D, Ryan A, Johnson R, Wu DK. Development of the mouse inner ear and origin of its sensory organs. Journal Of Neuroscience. 1998; 18:3327–3335. [PubMed: 9547240]

Oh SH, Johnson R, Wu DK. Differential expression of bone morphogenetic proteins in the developing vestibular and auditory sensory organs. J Neurosci. 1996; 16:6463–6475. [PubMed: 8815925]

Ohyama T, Basch ML, Mishina Y, Lyons KM, Segil N, Groves AK. BMP signaling is necessary for patterning the sensory and nonsensory regions of the developing mammalian cochlea. J Neurosci. 2010; 30:15044–15051. [PubMed: 21068310]

Pauley S, Wright TJ, Pirvola U, Ornitz D, Beisel K, Fritzsch B. Expression and function of FGF10 in mammalian inner ear development. Dev Dyn. 2003; 227:203–215. [PubMed: 12761848]

Phan KD, Hazen VM, Frendo M, Jia Z, Butler SJ. The bone morphogenetic protein roof plate chemorepellent regulates the rate of commissural axonal growth. J Neurosci. 2010; 30:15430–15440. [PubMed: 21084599]

Pirvola U, Spencer-Dene B, Xing-Qun L, Kettunen P, Thesleff I, Fritzsch B, Dickson C, Ylikoski J. FGF/FGFR-2(IIIb) signaling is essential for inner ear morphogenesis. J Neurosci. 2000; 20:6125–6134. [PubMed: 10934262]

Pirvola U, Ylikoski J, Trokovic R, Hebert JM, McConnell SK, Partanen J. FGFR1 is required for the development of the auditory sensory epithelium. Neuron. 2002; 35:671–680. [PubMed: 12194867]

Riccomagno MM, Martinu L, Mulheisen M, Wu DK, Epstein DJ. Specification of the mammalian cochlea is dependent on Sonic hedgehog. Genes Dev. 2002; 16:2365–2378. [PubMed: 12231626]

Riccomagno MM, Takada S, Epstein DJ. Wnt-dependent regulation of inner ear morphogenesis is balanced by the opposing and supporting roles of Shh. Genes Dev. 2005; 19:1612–1623. [PubMed: 15961523]

Sanchez-Calderon H, Francisco-Morcillo J, Martin-Partido G, Hidalgo-Sanchez M. Fgf19 expression patterns in the developing chick inner ear. Gene Expr Patterns. 2007; 7:30–38. [PubMed: 16798106]

Sanchez-Calderon H, Martin-Partido G, Hidalgo-Sanchez M. Otx2, Gbx2, and Fgf8 expression patterns in the chick developing inner ear and their possible roles in otic specification and early innervation. Gene Expr Patterns. 2004; 4:659–669. [PubMed: 15465488]

Sanchez-Camacho C, Bovolenta P. Emerging mechanisms in morphogen-mediated axon guidance. BioEssays. 2009; 31:1013–1025. [PubMed: 19705365]

Sapede D, Pujades C. Hedgehog signaling governs the development of otic sensory epithelium and its associated innervation in zebrafish. Journal of Neuroscience. 2010; 30:3612–3623. [PubMed: 20219995]

Tessarollo L, Coppola V, Fritzsch B. NT-3 replacement with brain-derived neurotrophic factor redirects vestibular nerve fibers to the cochlea. J Neurosci. 2004; 24:2575–2584. [PubMed: 15014133]

Webber A, Raz Y. Axon guidance cues in auditory development. Anat Rec A Discov Mol Cell Evol Biol. 2006; 288:390–396. [PubMed: 16550548]

Whitlon DS, Grover M, Tristano J, Williams T, Coulson MT. Culture conditions determine the prevalence of bipolar and monopolar neurons in cultures of dissociated spiral ganglion. Neuroscience. 2007; 146:833–840. [PubMed: 17331652]

Whitlon DS, Tieu D, Grover M, Reilly B, Coulson MT. Spontaneous association of glial cells with regrowing neurites in mixed cultures of dissociated spiral ganglia. Neuroscience. 2009; 161:227–235. [PubMed: 19324078]

Wright TJ, Mansour SL. FGF signaling in ear development and innervation. Curr Top Dev Biol. 2003; 57:225–259. [PubMed: 14674483]

Wu DK, Oh SH. Sensory organ generation in the chick inner ear. J Neurosci. 1996; 16:6454–6462. [PubMed: 8815924]

Yang T, Kersigo J, Jahan I, Pan N, Fritzsch B. The molecular basis of making spiral ganglion neurons and connecting them to hair cells of the organ of Corti. Hear Res. 2011; 278:21–33. [PubMed: 21414397]

Zimmerman LB, De Jesus-Escobar JM, Harland RM. The Spemann organizer signal noggin binds and inactivates bone morphogenetic protein 4. Cell. 1996; 86:599–606. [PubMed: 8752214]

Zou Y, Lyuksyutova AI. Morphogens as conserved axon guidance cues. Current Opinion in Neurobiology. 2007; 17:22–28. [PubMed: 17267201]

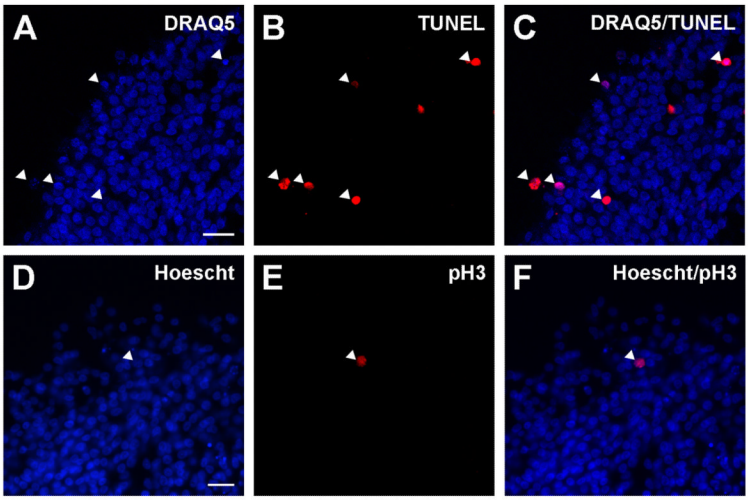

Figure 1.

Representative example of TUNEL and pH3 staining on cryosections of SAG explants in collagen gels.

Upper and lower panels show TUNEL labeling and pH3 immunohistochemistry, respectively. Confocal images of sections labeled with DRAQ5 (A) and TUNEL (B). Images of DRAQ5 and TUNEL staining merged for cell death quantification (C). Far-red DRAQ5 images were false-colored as blue. The percentage of TUNEL-positive neurons was calculated by dividing the number of DRAQ5/TUNEL double-positive cells (arrowheads in C) by the total number of DRAQ5 cells. Images of Hoescht counter-staining (D) and pH3 immunostaining (E). Images of Hoescht and pH3 staining merged (F). The percentage of proliferating cells was calculated by dividing the number of pH3/Hoescht double-positive cells (arrowhead in C) by the total number of Hoescht-labeled cells.

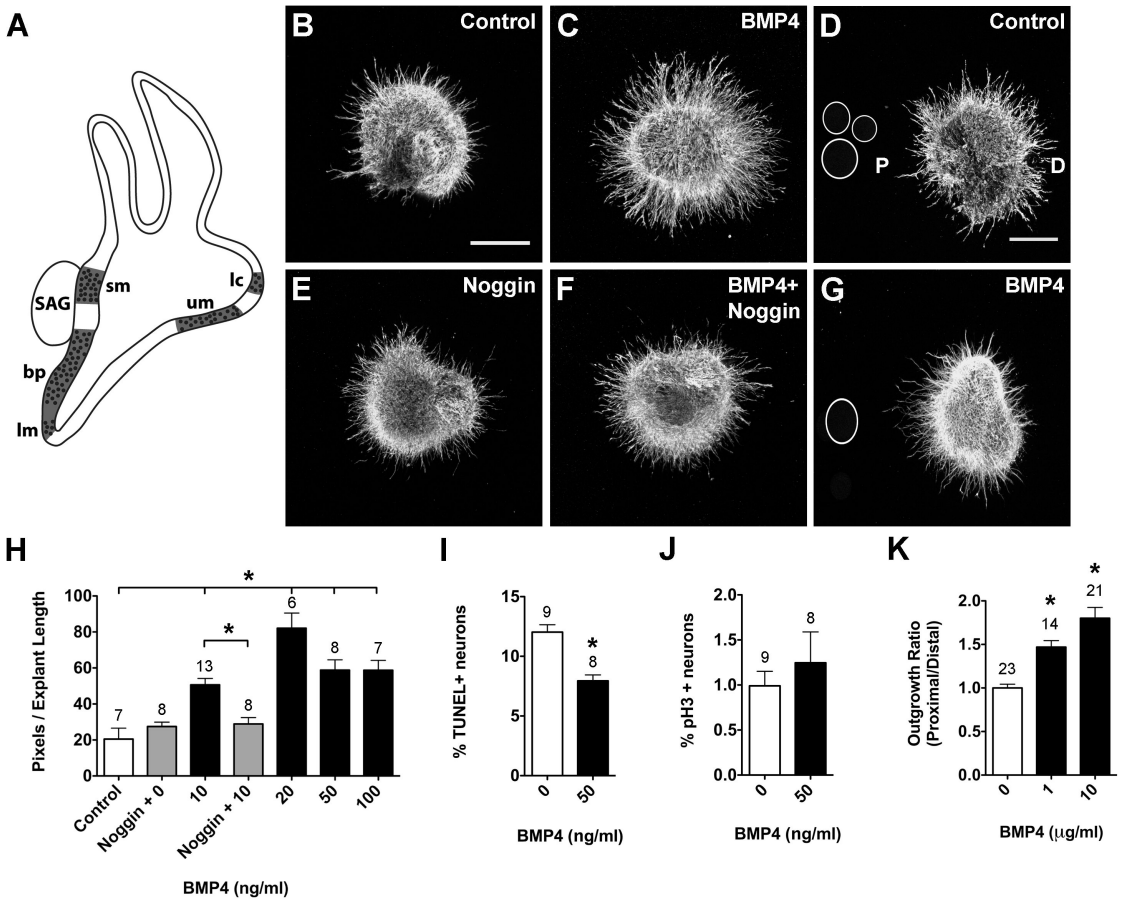

Figure 2.

BMP4 promotes neuron survival and neurite outgrowth in HH20-25 SAGs cultured for 24 hours.

Summarized expression of Bmp4 transcripts (A) in the developing chick inner ear during stages of SAG neuron axon pathfinding and sensory organ innervation; based on (Wu and Oh, 1996). Prosensory regions are represented by dotted areas (here and in subsequent figures) and include the basilar papilla (bp), lateral crista (lc), lagena macula (lm), saccular macula (sm) and utricular macula (um). SAG explants cultured with vehicle (Control; B), 10 ng/ml BMP4 (C), 1 μg/ml Noggin (E), or 10 ng/ml BMP4 plus 1 μg/ml Noggin (E). SAG explants co-cultured with beads soaked in PBS (Control; D) or 10 μg/ml BMP4 (G). Scale bar = 200 μm. Quantification of the average pixel number for protein-treated SAG explants (H), the percentage of TUNEL positive SAG neurons (I) and the mitotic index of SAG neurons (J). Quantification of neurite outgrowth for SAG-bead co-cultures (K). In all figures, the following labeling conventions are used: bars represent the mean (±SE) computed from explants within a treatment group; sample numbers for each treatment group are above the bars; the outgrowth ratio is the average proximal/distal ratio of pixels per explant length for SAG-bead co-cultures with D as distal quadrant and P as proximal quadrant. In this figure, *$p < 0.0001$ significantly different from controls.

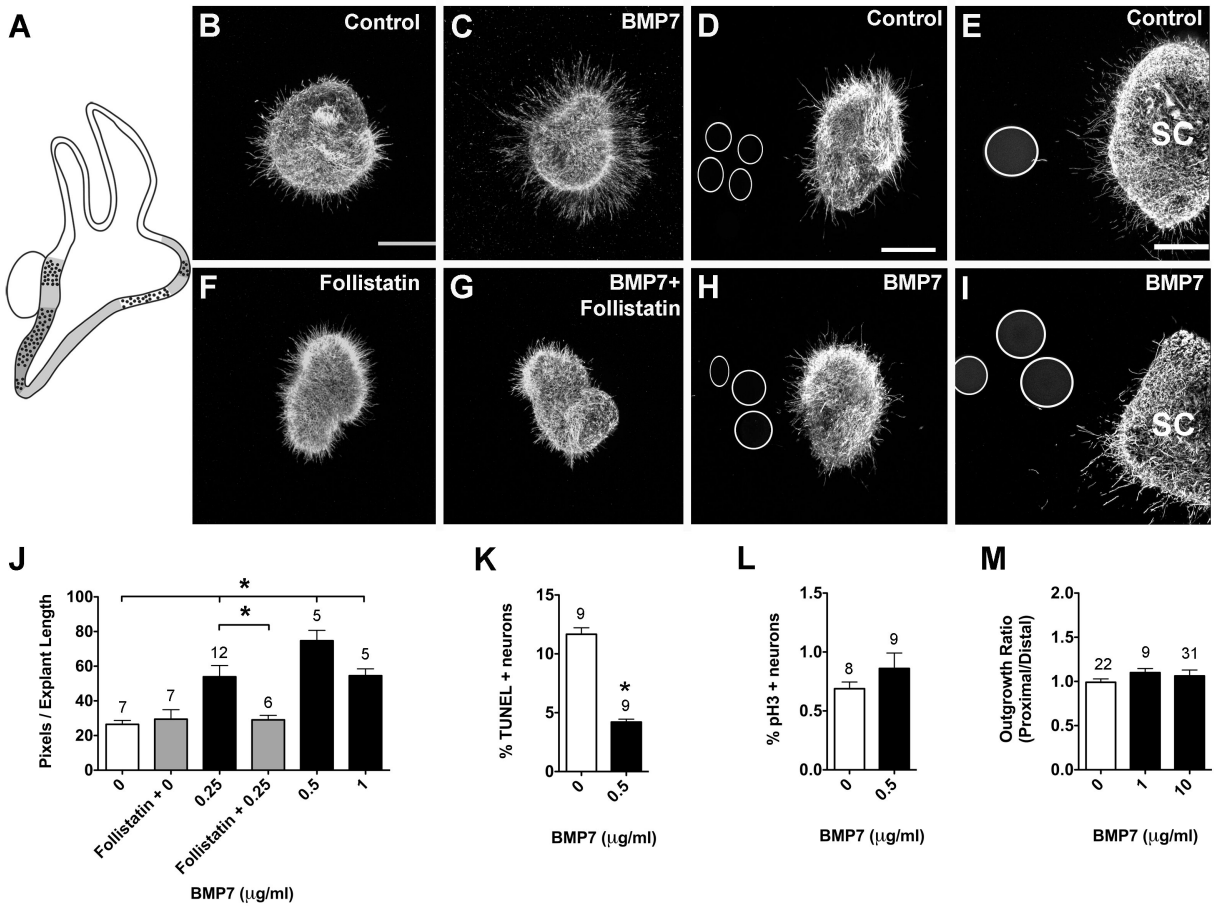

Figure 3.

BMP7 promotes neurite outgrowth and neuron survival in HH20-25 SAGs cultured for 24 hours.

Summarized expression patterns of Bmp7 transcripts (A). At HH24, Bmp7 expression is diffuse, based on (Oh et al., 1996) and overlaps with Bmp4 expression (1A). SAG explants cultured with vehicle (Control; B), 0.25 μg/ml BMP7 (C), 2 μg/ml Follistatin (F), or 0.25 μg/ml BMP7 plus 2 μg/ml Follistatin (G). SAG explants co-cultured with beads soaked in PBS (Control; D) or 10 μg/ml BMP7 (H). E4 (HH24-25) spinal cord explants co-cultured with PBS (E) or 10 μg/ml BMP7-treated beads (I). Scale bar = 200 μm. Quantification of the average pixel number for protein-treated SAG explants (J), the percentage of TUNEL positive neurons (K) and the mitotic index (L). Quantification of neurite outgrowth for SAG-bead co-cultures (M). See legend to figure 1 for labeling conventions. SC, spinal cord. *p <0.0001 significantly different from controls.

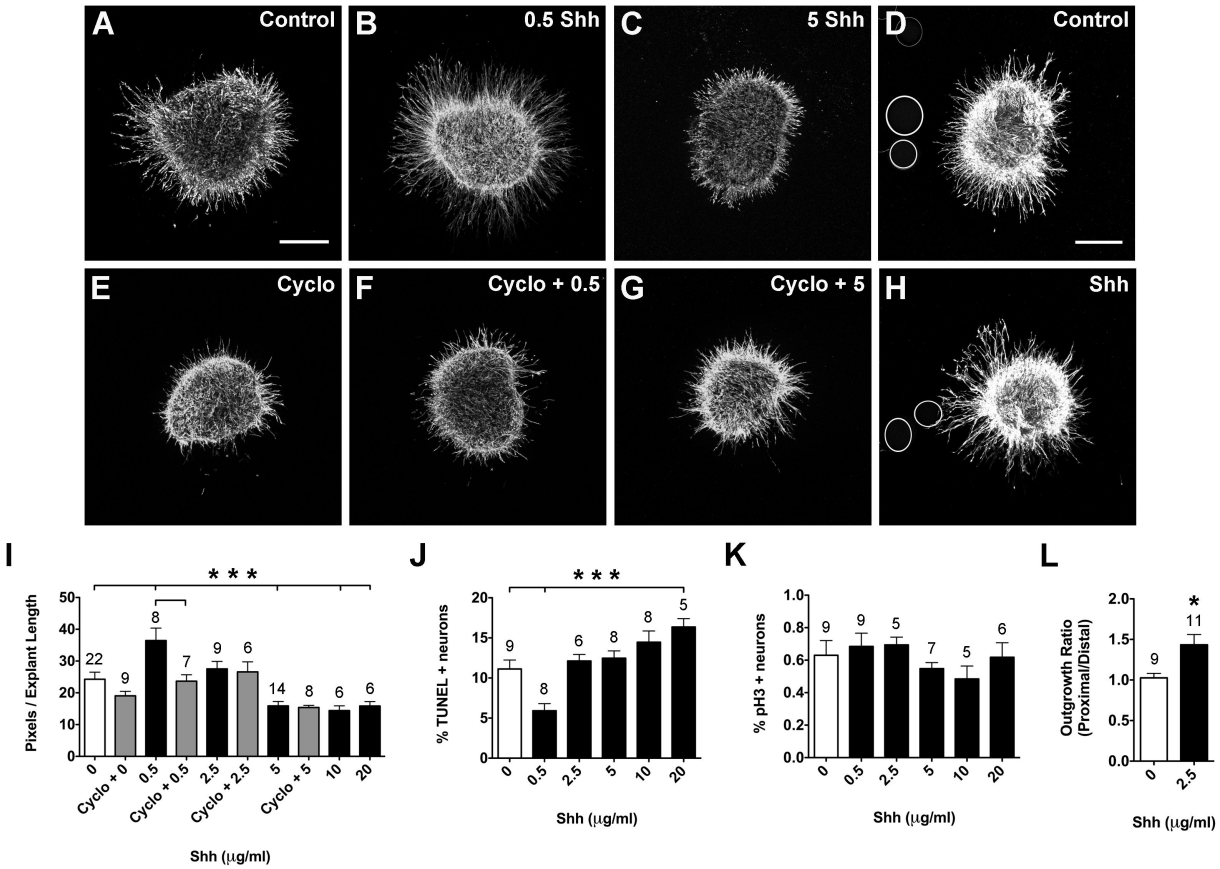

Figure 4.

Shh promotes neuron survival and neurite outgrowth in HH20-25 SAGs cultured for 24 hours.

SAG explants cultured with vehicle (Control; A), 0.5 μg/ml Shh (B), 5 μg/ml Shh (C), 10 μM Cyclopamine (E), 0.5 μg/ml Shh plus 10 μM Cyclopamine (F), or 5 μg/ml Shh+ 10 μM Cyclopamine (G). SAG explants co-cultured with beads soaked in PBS (Control; D) or 2.5 μg/ml Shh (H). Scale bar = 200 μm. Quantification of the average pixel number for SAG explants (I), the percentage of TUNEL positive neurons (J) and the mitotic index (K). Quantification of neurite outgrowth for SAG-bead co-cultures (L). See legend to figure 1 for labeling conventions.

***p<0.0001 and *p<0.05 significantly different from controls.

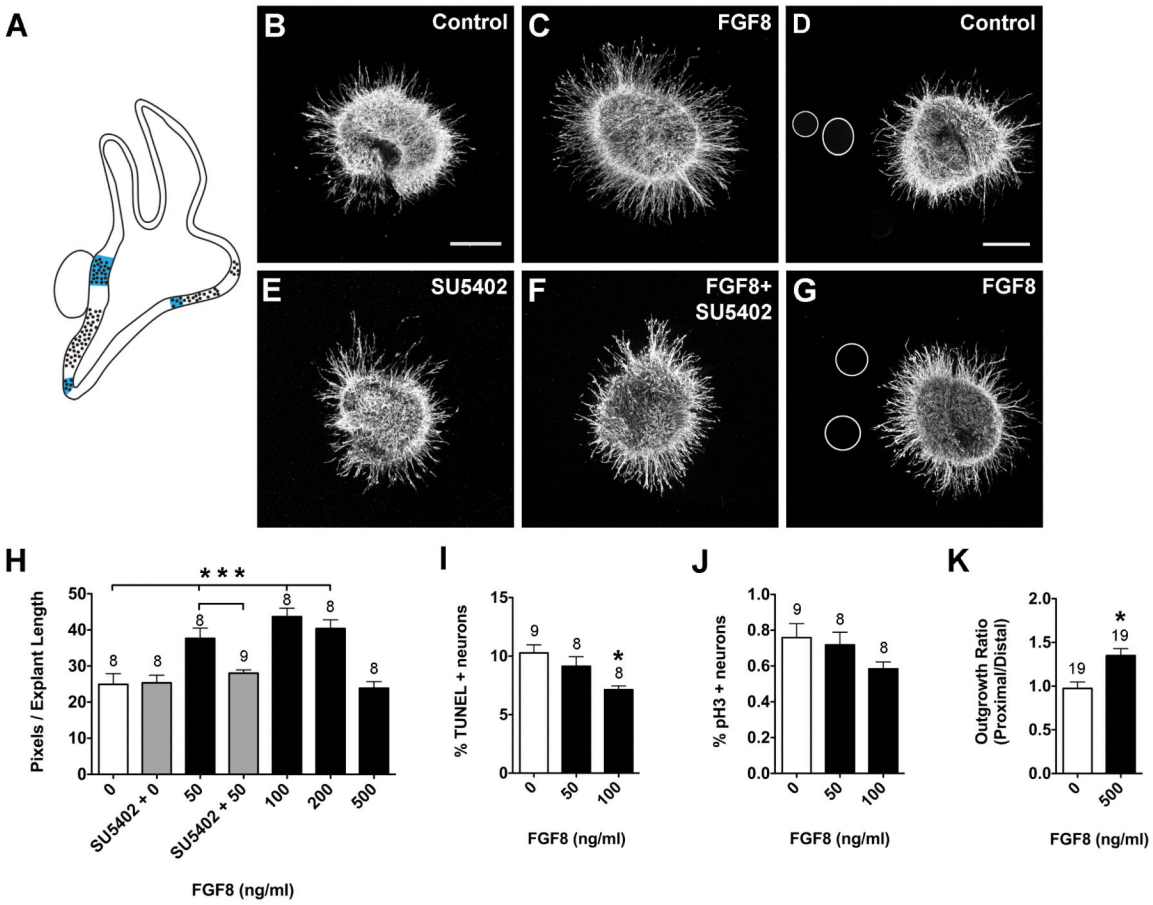

Figure 5.

FGF8 promotes neuron survival and neurite outgrowth in HH20-25 SAGs cultured for 24 hours.

Summarized expression patterns of Fgf8 transcripts (A). Fgf8 transcripts are expressed in the innervated saccular macula and lagena macula and part of the utricular macula, based on (Sanchez-Calderon et al., 2004). SAG explants cultured with vehicle (Control; B), 50 ng/ml FGF8 (C), 0.1 μM SU5402 (E), or 50 ng/ml FGF8 plus 0.1 μM SU5402 (F). SAG explants co-cultured with beads soaked in PBS (D) or 500 ng/ml FGF8 (G). Scale bar = 200 μm. Quantification of the average pixel number for SAG explants (H), the percentage of TUNEL positive neurons (I) and the mitotic index (J). Quantification of neurite outgrowth for SAG-bead co-cultures (K). See legend to figure 1 for labeling conventions. ***p<0.0001 and *p<0.01 significantly different from controls.

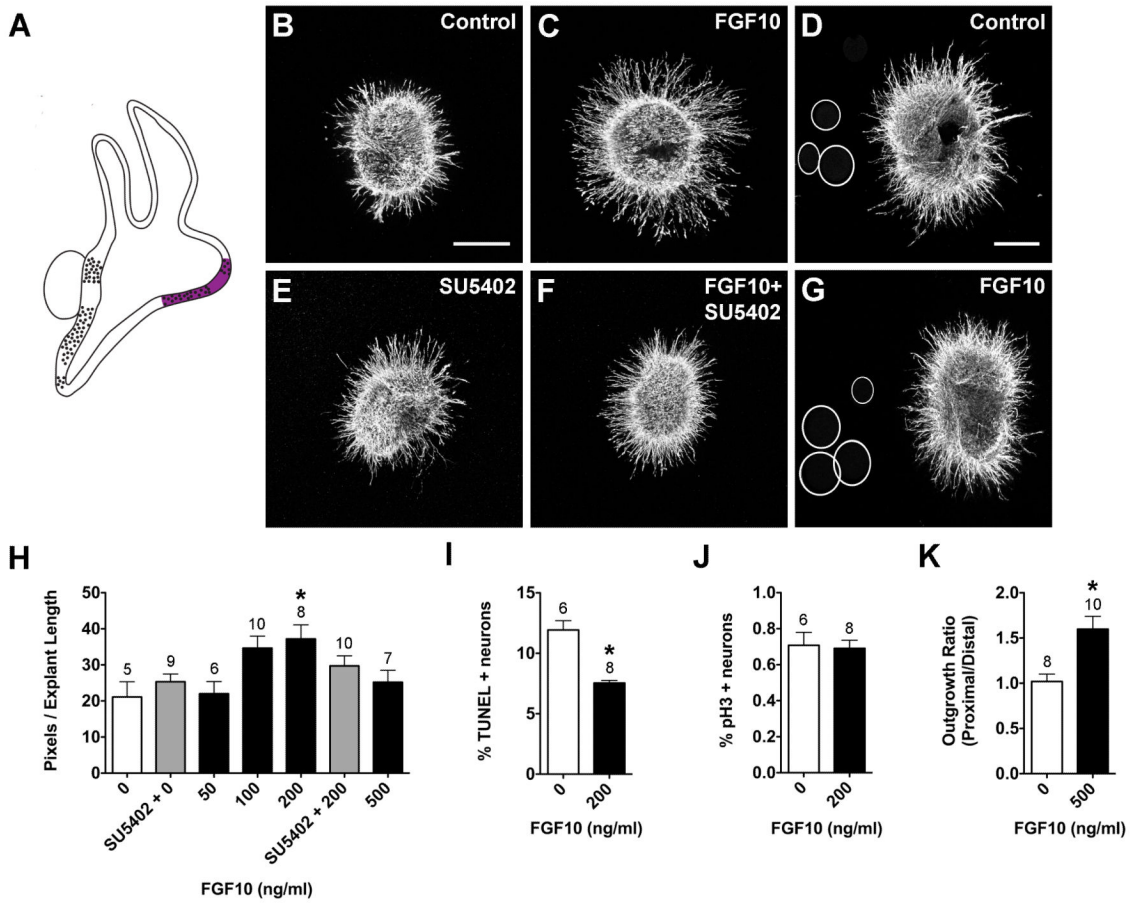

Figure 6.

FGF10 promotes neuron survival and neurite outgrowth in HH20-25 SAGs cultured for 24 hours.

Summarized expression of Fgf10 transcripts (A) in the developing chick inner ear at HH26 (A). FGF10 transcripts are expressed in the anterior, lateral, and posterior (not shown) cristae and the utricular macula, based on (Chang et al. 2004). SAG explants cultured with vehicle (Control; B), 200 ng/ml FGF10 (C), 0.1 μM SU5402 (E), or 200 ng/ml FGF10 plus 0.1 μM SU5402 (F). SAG co-cultures with beads soaked in PBS (D) or 500 ng/ml FGF10 (G). Scale bar = 200 μm. Quantification of the average pixel number for SAG explants (H), the percentage of TUNEL positive neurons (I) and the mitotic index (J). Quantification of neurite outgrowth for SAG-bead co-cultures (K). See legend to figure 1 for labeling conventions. *p<0.01 significantly different from controls.

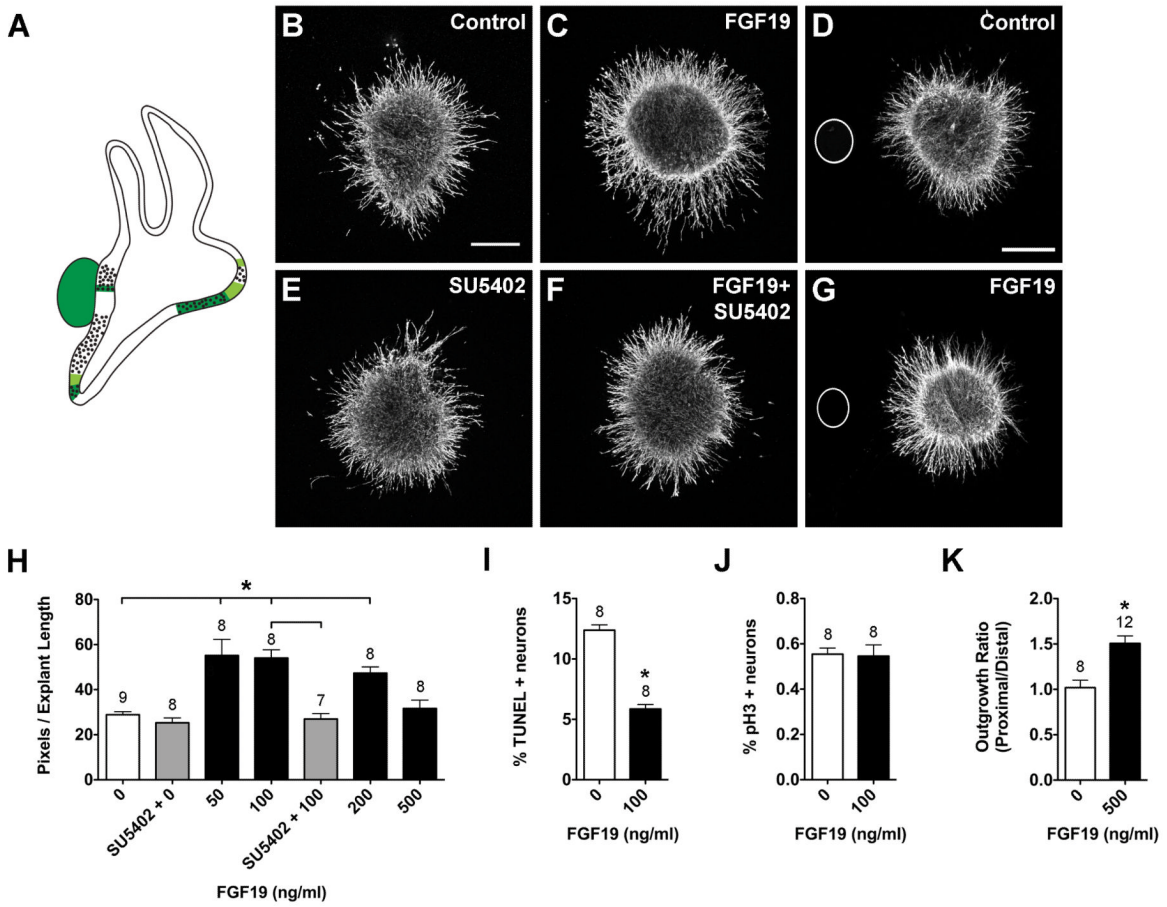

Figure 7.

FGF19 promotes neuron survival and neurite outgrowth in HH20-25 SAGs cultured for 24 hours.

Summarized expression patterns of Fgf19 transcripts (A). Fgf19 is strongly expressed in the utricular macula, lagena macula, SAG, and displays weaker expression in some of the prosensory region borders, based on (Sanchez-Calderon et al., 2007). SAG explants cultured with vehicle (Control; B), 100 ng/ml FGF19 (C), 0.1 μM SU5402 (E), or 100 ng/ml FGF19 plus 0.1 μM SU5402 (F). SAG explants co-cultured with beads soaked in PBS (D) or 500 ng/ml FGF19 (G). Scale bar = 200 μm. Quantification of the average pixel number for SAG explants (H), the percentage of TUNEL positive neurons (I) and the mitotic index (J). Quantification of neurite outgrowth for SAG-bead co-cultures (K). See legend to figure 1 for labeling conventions. *p<0.0001 significantly different from controls.

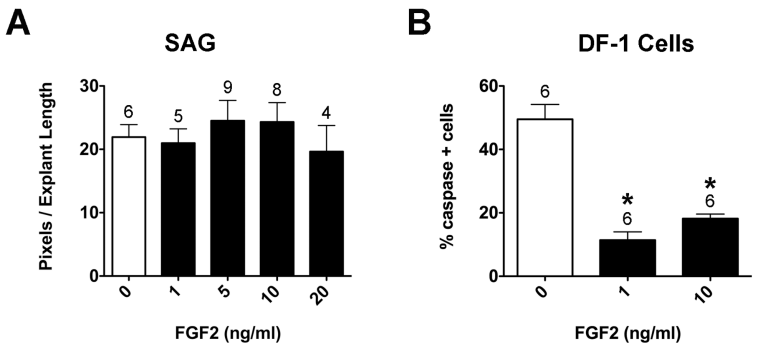

Figure 8.

Purified human FGF2 does not affect neurite outgrowth in HH20-25 SAGs cultured for 24 hours.

Quantification of the average pixel number for SAG explants (A) and the percentage of caspase-3 positive DF1 cells (B). No significant difference in pixel number was found between control and 1-20 ng/ml FGF2 treated explants (A; ANOVA, $p=0.7874$). There were significantly fewer caspase-3 positive DF-1 cells in the presence of 1 and 10 ng/ml FGF2 compared to controls (B; ANOVA, $p<0.0001$), demonstrating that the purified FGF2 protein used in the SAG experiments is bioactive.